JCB Article

ADP ribosylation factor 6 is activated and controls membrane delivery during phagocytosis in macrophages

Florence Niedergang,[1] Emma Colucci-Guyon,[1] Thierry Dubois,[1] Graça Raposo,[2] and Philippe Chavrier[1]

[1]Membrane and Cytoskeleton Dynamics Group and [2]Electron Microscopy Group, UMR 144 Centre National de la Recherche Scientifique, Institut Curie, F-75248 Paris Cedex 05, France

Engulfment of particles by phagocytes is induced by their interaction with specific receptors on the cell surface, which leads to actin polymerization and the extension of membrane protrusions to form a closed phagosome. Membrane delivery from internal pools is considered to play an important role in pseudopod extension during phagocytosis. Here, we report that endogenous ADP ribosylation factor 6 (ARF6), a small GTP-binding protein, undergoes a sharp and transient activation in macrophages when phagocytosis was initiated via receptors for the Fc portion of immunoglobulins (FcRs). A dominant-negative mutant of ARF6 (T27N mutation) dramatically affected FcR-mediated phagocytosis. Expression of ARF6-T27N lead to a reduction in the focal delivery of vesicle-associated membrane protein 3^+ endosomal recycling membranes at phagocytosis sites, whereas actin polymerization was unimpaired. This resulted in an early blockade in pseudopod extension and accumulation of intracellular vesicles, as observed by electron microscopy. We conclude that ARF6 is a major regulator of membrane recycling during phagocytosis.

Introduction

Phagocytosis is the mechanism of internalization used by cells to take up relatively large particles (>0.5 μm) into an intracellular compartment or phagosome. Professional phagocytes, like macrophages, polymorphonuclear granulocytes, and dendritic cells, use it to internalize and degrade microorganisms, cell debris, and diverse particulates (Aderem and Underhill, 1999). Phagocytosis is triggered by the recognition of ligands exposed on the particle surface by specific receptors or lectins present on the phagocyte surface. The clustering of receptors is followed by a cascade of activation that is best described for receptors for the Fc portion of immunoglobulins (FcRs;* Greenberg and Grinstein, 2002). FcR signaling involves tyrosine kinases, and eventually leads to the formation of pseudopods that engulf the particle. It is generally considered that actin polymerization provides the driving force that allows the plasma membrane to be locally elongated to form the engulfing pseudopods (Castellano et al., 2001; May and Machesky, 2001).

Simultaneous internalization of multiple particles in phagosomes should result in a decrease in the net surface of macrophages, yet, the macrophage surface rather increases during phagocytosis (Hackam et al., 1998; Holevinsky and Nelson, 1998). Exocytosis of membranes from internal compartments has been proposed as a compensatory mechanism for surface loss (Booth et al., 2001; Aderem, 2002). In particular, endocytic vesicles bearing the vesicle-associated membrane protein 3 (VAMP3) marker have been shown to be delivered at the site of phagocytosis (Bajno et al., 2000). However, in contrast to extensive knowledge about actin polymerization, the activation cascade leading to focal membrane delivery is largely unknown.

The small GTP-binding protein ADP ribosylation factor 6 (ARF6) belongs to the ARF family of Ras-related GTP-binding proteins. It is involved in membrane trafficking during receptor-mediated endocytosis, endosomal recycling, and exocytosis of secretory granules (D'Souza-Schorey et al., 1995, 1998; Radhakrishna and Donaldson, 1997; Vitale et al., 2002). ARF6 has also been implicated in the formation of actin-rich membrane protrusions and ruffles (Radhakrishna et al., 1996). In addition, ARF6 was shown to play a role in phagocytosis because both a constitutively active and a

Address correspondence to Florence Niedergang, Membrane and Cytoskeleton Dynamics Laboratory, UMR144 CNRS, Institut Curie, 26 rue d'Ulm, F-75248 Paris cedex 05, France. Tel.: 33-1-42-34-63-67. Fax: 33-1-42-34-63-77. E-mail: Florence.Niedergang@curie.fr

*Abbreviations used in this paper: ARF, ADP ribosylation factor; FcR, receptor for the Fc portion of immunoglobulins; GGA, Golgi-localized γ ear–containing ARF-binding protein; PI3K, phosphatidylinositol 3-kinase; SRBC, sheep red blood cell; Tf, transferrin; VAMP, vesicle-associated membrane protein; WT, wild type.

Key words: VAMP3/cellubrevin; ARF6; recycling; endocytosis; actin

The Journal of Cell Biology, Volume 161, Number 6, June 23, 2003 1143–1150
http://www.jcb.org/cgi/doi/10.1083/jcb.200210069

dominant-negative form of the protein inhibited phagocytosis (Zhang et al., 1998). However, the precise function of ARF6 in phagocytosis remains largely unknown. Here, we show that endogenous ARF6 becomes activated very early and transiently during FcR-mediated phagocytosis in murine macrophages, and plays a critical role in the delivery of membrane from recycling compartments to the forming phagosome.

Results

ARF6 is transiently activated during FcR-mediated phagocytosis

Murine macrophages from the RAW264.7 line transiently expressing wild-type (WT) and dominant-negative (T27N mutant) ARF6 were incubated with IgG-opsonized sheep red blood cells (IgG-SRBCs) for 60 min at 37°C, and the efficiency of phagocytosis was assessed. As shown in Fig. 1 A, the association of opsonized particles to macrophages was not affected by either construct. In contrast, expression of ARF6-T27N strongly decreased the efficiency of FcR-dependent phagocytosis, whereas ARF6-WT had virtually no effect (Fig. 1 B).

These results confirmed previous data (Zhang et al., 1998) and pointed to an essential role of ARF6 in the phagocytic process. We have now monitored the activation level of endogenous ARF6 during phagocytosis. GTP-loaded ARF6 was detected by a GST pull-down assay based on GST fused to the ARF-binding domain of Golgi-localized γ ear–containing ARF-binding protein 3 (GGA3; Santy and Casanova, 2001). The activation of ARF6 was observed in RAW264.7 macrophages at times as short as 1 min, reaching a maximum at 10 min, and decreasing later to return to basal level after 30 min (Fig. 1 C). No precipitation of ARF6 was ever detected when GST alone was added in the pull-down assay, and aliquots of the total lysates indicated that the variations observed after precipitation were not due to variations in the total amount of proteins (Fig. 1 C). Because Rac and Cdc42 are crucial for FcR-mediated phagocytosis, their activation was monitored under the same conditions (Fig. 1 D). While the kinetics of activation of Cdc42 was comparable to that observed for ARF6, the activation of Rac peaked 1 min after the contact of macrophages with particles and then decreased. Therefore, Rac is activated before ARF6 and Cdc42 during FcR-mediated phagocytosis in RAW264.7 cells.

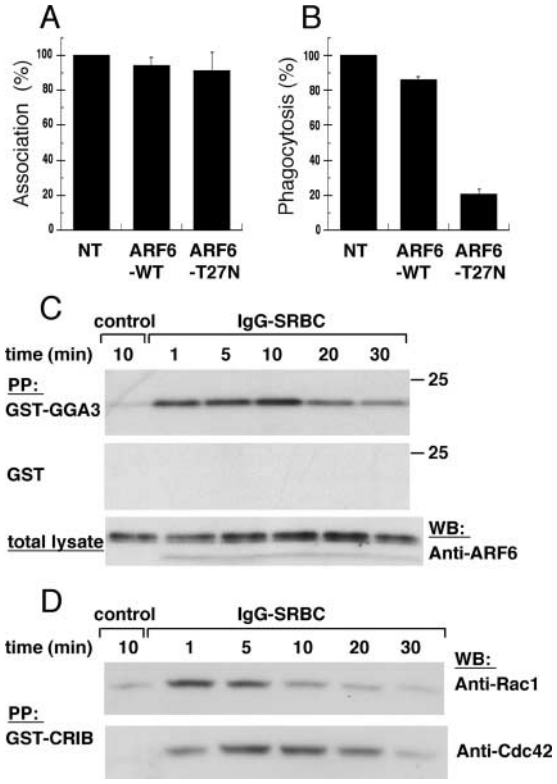

Figure 1. **ARF6 is activated during phagocytosis.** RAW264.7 macrophages transiently expressing ARF6-WT or ARF6-T27N were incubated with IgG-SRBC for 60 min at 37°C. The cells were fixed, and external SRBCs were stained with Cy3-coupled anti–rabbit IgG antibodies. After permeabilization, the expressed HA-tagged ARF6 constructs were detected by immunofluorescence. The efficiency of association (A) or phagocytosis (B) was calculated as indicated in Materials and methods. The mean ± SEM of three independent experiments is plotted. NT, non transfected. (C) ARF6 is transiently activated during phagocytosis. RAW264.7 macrophages were incubated with medium (control) for 10 min or with IgG-SRBC for various times at 37°C. Lysates were prepared and incubated with GST-GGA3$_{1–226}$ (top) or GST alone (middle). The bottom panel shows aliquots of total lysates. Western blot was performed with anti-ARF6 antibodies. Data are representative of three experiments. (D) Kinetics of activation of Rac and Cdc42 during phagocytosis. RAW264.7 macrophages were activated as described in C, and lysates were prepared and incubated with GST-CRIB. Western blot was performed with anti-Rac antibodies (top), then with anti-Cdc42 (bottom). Data are representative of four experiments.

Inhibition of receptor-mediated endocytosis does not impair the efficiency of phagocytosis

Because ARF6 controls clathrin-mediated endocytosis in some cell types (D'Souza-Schorey et al., 1995; Altschuler et al., 1999; Palacios et al., 2001), the inhibition of phagocytosis by dominant-negative ARF6 could be the consequence of an inhibition of endocytosis in the transfected macrophages. To test this, we specifically blocked clathrin-mediated endocytosis with a mutant of Eps15, a protein that binds AP2 and is targeted to clathrin-coated pits (Benmerah et al., 2000). As previously shown in fibroblasts (Benmerah et al., 2000), expression of the DIII domain of Eps15, which prevents clathrin coat assembly, inhibited transferrin (Tf) uptake in RAW264.7 cells. The DIIIΔ2 construct that does not contain the AP2-binding sites and was used as a control did not inhibit endocytosis (Fig. 2 A). Neither construct affected phagocytosis of IgG-SRBCs (Fig. 2, B and C). These results clearly demonstrate that blocking receptor-mediated endocytosis is not sufficient to inhibit phagocytosis.

Dominant-negative ARF6 inhibits membrane recruitment (but not actin polymerization) at the site of phagocytosis

Endocytic vesicles positive for VAMP3 are recruited and exocytosed at the site of phagocytosis (Bajno et al., 2000). Because ARF6 has been shown to colocalize with VAMP3 in endosomal vesicles (D'Souza-Schorey et al., 1998) and has been involved in membrane recycling from the endocytic

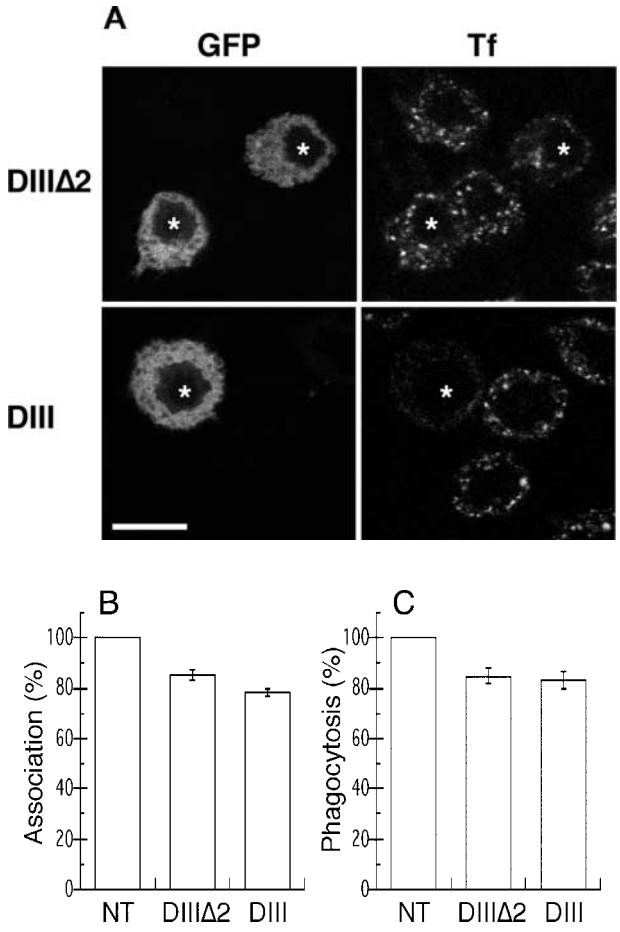

Figure 2. **An Eps15 mutant inhibits Tf endocytosis but not FcR-mediated phagocytosis.** RAW264.7 cells transiently expressing GFP-Eps15DIIIΔ2 (top) or the dominant-negative construct GFP-Eps15DIII (bottom) were incubated for 30 min at 37°C in medium containing 60 nM Texas red-Tf. Cells were then fixed and analyzed by confocal microscopy. A medial optical section is shown. Left, GFP; right, Texas red-Tf. The asterisks indicate GFP-positive transfected cells. Bar, 10 μm. (B and C) Inhibition of receptor-mediated endocytosis does not block phagocytosis. Association (B) and phagocytic (C) efficiency of cells expressing GFP-Eps15DIIIΔ2 or GFP-Eps15DIII were compared with the efficiency of phagocytosis of nontransfected (NT) control cells, as described in Fig. 1 and Materials and methods. Data presented are the mean ± SEM of three independent experiments.

compartment (D'Souza-Schorey et al., 1995; Radhakrishna and Donaldson, 1997), we reasoned that ARF6 may be implicated in the recycling and delivery of membranes to nascent phagosomes. To test this hypothesis, we analyzed the effect of the expression of ARF6-WT or ARF6-T27N on the recruitment of VAMP3 at the site of phagocytosis in RAW264.7 macrophages. Accumulations of GFP-VAMP3 (Fig. 3, B and F) and polymerized actin filaments (Fig. 3, C and G) were scored 10 min after the addition of IgG-SRBCs (Fig. 3 I). The expression of ARF6-WT and ARF6-T27N resulted in a small reduction of F-actin accumulation compared with controls, whereas only ARF6-T27N lead to a strong reduction in the recruitment of GFP-VAMP3 around SRBCs (Fig. 3 F, arrowhead; Fig. 3 I). Inhibition of phosphatidylinositol 3-kinase (PI3K) was shown to block phagocytosis (Araki et al., 1996; Cox et al., 1999; unpublished data). Therefore, we also analyzed accumulations of GFP-VAMP3 and F-actin in cells treated with wortmannin to inhibit PI3K. Compared with DMSO-treated control cells, cells incubated with wortmannin showed a reduced recruitment of GFP-VAMP3, whereas the presence of F-actin cups was increased (Fig. 3 J). These results show that ARF6 plays an essential role in membrane recruitment around the phagocytosed particle, with little (if any) effect on actin assembly. Next, we quantified by flow cytometry the amount of F-actin in ARF6-WT– or ARF6-T27N–expressing cells at different time points during phagocytosis. As reported earlier, the amount of F-actin increased on contact with the particles (by 20–50%, depending on the experiments), peaked at 2.5–10 min, and decreased (unpublished data; Coppolino et al., 2002). Compared with ARF6-WT, expression of dominant-negative ARF6 resulted in a small decrease in F-actin at any of the time points analyzed (Fig. 3 K), which confirms the results obtained by scoring under the microscope (Fig. 3 I). Together, these results indicate that membrane delivery, rather than actin polymerization, is under the control of ARF6 during phagocytosis.

Dominant-negative ARF6 inhibits membrane recycling and pseudopod extension

To characterize the role of ARF6 in membrane recruitment, we followed by flow cytometry the kinetics of recycling of Alexa® 633–labeled Tf in RAW264.7 macrophages coexpressing ARF6-T27N and GFP (Fig. 4 A). Tf is constitutively endocytosed and recycled with its receptor via a VAMP3-positive recycling compartment (Dautry-Varsat et al., 1983; Bajno et al., 2000). In control GFP-negative cells or in cells expressing GFP alone, Tf recycling was rapid (Fig. 4 A), as reported earlier in macrophages (Cox et al., 2000). By contrast, the efflux of Tf was clearly reduced in cells expressing ARF6-T27N (Fig. 4 A). This shows that ARF6 is able to modulate the constitutive recycling of Tf in macrophages. Then, we examined phagocytosing ARF6-T27N–expressing cells at the ultrastructural level. An accumulation of large electronlucent vesicles was observed in these cells as compared with cells expressing ARF6-WT (Fig. 4 B). Large vesicles were present in ~80% of the ARF6-T27N–positive cells that were in contact with at least one SRBC, whereas they were observed in <20% of the ARF6-WT–expressing cells bound to SRBCs. The enlarged compartments observed in ARF6-T27N cells sometimes contained internal membranes (Fig. 4 B, arrowheads). All together, these results indicate that mutated ARF6 interferes with the recycling pathway followed by the Tf receptors, as well as with the delivery of membranes to the site of phagocytosis.

To get further insight into the stage of phagocytosis that is affected by dominant-negative ARF6, transfected macrophages were analyzed by scanning EM at different times of phagocytosis. After 10 min, opsonized SRBCs were associated with the surface of the macrophages expressing ARF6-WT or ARF6-T27N, and membrane extensions were observed around the particle (Fig. 5, A and B). After 60 min, ARF6-WT–expressing cells were spread and showed extensive membrane ruffles, and all particles had been internalized

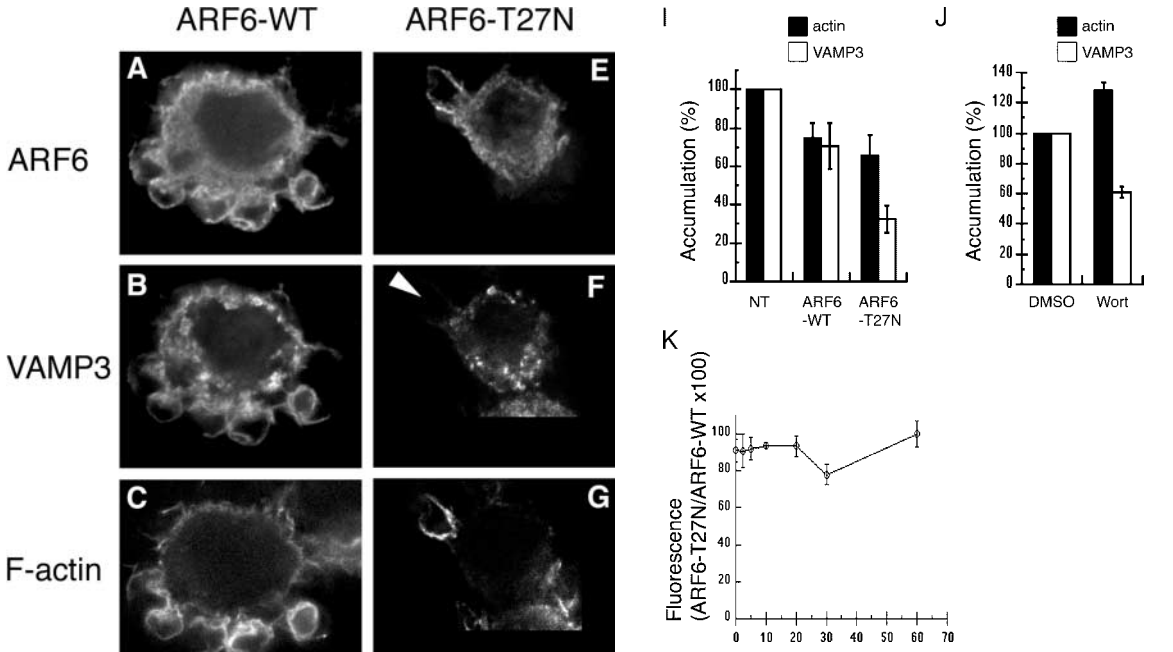

Figure 3. **ARF6-T27N inhibits the recruitment of VAMP3 (but not the polymerization of actin) at the site of phagocytosis.** RAW264.7 cells stably expressing GFP-VAMP3 (B and F) were transiently transfected to express ARF6-WT-HA (A–D) or ARF6-T27N-HA (E–H) and were incubated with Cy5-IgG-SRBC (D and H) for 10 min at 37°C. The cells were then permeabilized and stained with Alexa® 350-phalloidin (C and G) to detect F-actin, and anti-HA followed by Cy3-labeled anti–rat IgG (A and E) to reveal HA-tagged ARF6. Cells were analyzed by conventional epifluorescence microscopy and deconvolution. One section is shown. Bar, 10 μm. Accumulations of GFP-VAMP3 (open bars) and polymerized actin (filled bars) were scored as described in Materials and methods for ARF6-WT– and ARF6-T27N–expressing cells (I) or for wortmannin-treated cells (J), and expressed as a percentage of the indexes obtained for control nontransfected (NT) cells (I) or DMSO-treated cells (J). Data are the mean ± SEM of at least four independent experiments performed with two different stable clones. Flow cytometry quantification of polymerized actin during phagocytosis (K). RAW264.7 cells positive for GFP, coexpressed with ARF6-WT or ARF6-T27N, were incubated with IgG-SRBC at 37°C and, at different time points, fixed, permeabilized, and stained with Alexa® 633–phalloidin. The levels of fluorescence were then measured by FACS® on at least 5,000 positive cells. The F-actin content of ARF6-T27N–expressing cells was then expressed as a percentage of the values obtained for ARF6-WT–expressing cells. Data are the mean ± SEM of four independent experiments performed.

(Fig. 5 C). In contrast, SRBCs were still extracellular on cells expressing ARF6-T27N (Fig. 5, D–F). In these cells, the pseudopods did not extend all around the particles bound to the macrophage surface. Only small extensions of membrane or pedestal-like structures were formed (Fig. 5 D, arrowhead; Fig. 5, E and F). These observations confirmed that phagocytosis was blocked at an early stage in cells expressing ARF6-T27N, before the formation and complete closure of the phagosome.

Discussion

In this paper, we have shown that endogenous ARF6 is activated early during FcR-mediated phagocytosis in macrophages, and that GTP-bound ARF6 controls the delivery of membrane from the endocytic recycling compartment to allow pseudopod extension.

ARF6 was shown to control clathrin-coated pits-mediated endocytosis in different systems (D'Souza-Schorey et al., 1995; Altschuler et al., 1999; Palacios et al., 2001). Therefore, the inhibition of phagocytosis by the dominant-negative ARF6 could have resulted from a more general blockade of endocytosis. We could rule out this possibility because a mutant of Eps15 (Benmerah et al., 2000) that is considered as the most specific tool to block clathrin-mediated endocytosis had no effect on FcR-dependent phagocytosis. Indeed, a link between phagocytosis and receptor-mediated endocytosis had been suggested earlier because clathrin-coated pit-associated proteins, as well as dynamin 2 and amphiphysin IIm, which are key regulators of receptor-mediated endocytosis, were also involved in phagocytosis (Gold et al., 1999, 2000; Perry et al., 1999). Our data show now that blocking receptor-mediated endocytosis is not sufficient to inhibit phagocytosis, which is in favor of specific roles for dynamin and amphiphysin in phagocytosis (Tse et al., 2003) that differ from clathrin-coated pit formation (i.e., membrane extension around the phagosome, actin polymerization, or scission of the closed vesicle).

A previous report proposed a role for ARF6 in actin dynamics during phagocytosis, based on the default in actin cup formation in macrophages expressing ARF6-T27N (Zhang et al., 1998). However, our data demonstrate that ARF6 con-

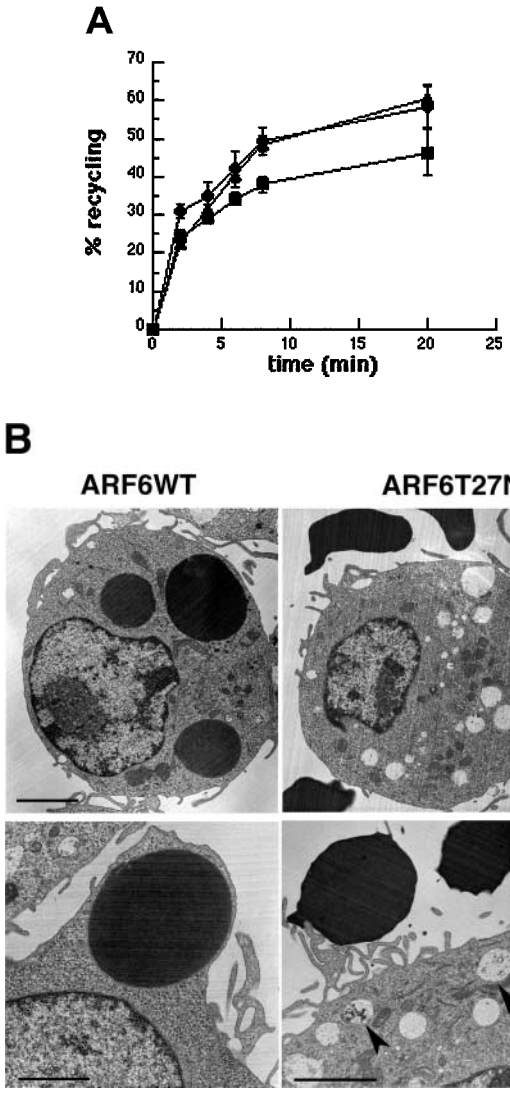

Figure 4. **Dominant-negative ARF6 inhibits membrane recycling.** Macrophages transiently coexpressing ARF6-T27N and GFP or GFP alone were scraped, pelleted, and resuspended in the presence of Alexa® 633-Tf for 45 min at 37°C. The efflux of Tf was then followed by flow cytometry as described in Materials and methods. Cells positive for GFP coexpressed with ARF6-T27N (closed squares), cells expressing GFP alone (closed circles), as well as cells negative for GFP (closed triangles) were gated and analyzed. The plot represents the mean ± SEM of three independent experiments. (B) Macrophages expressing ARF6-T27N accumulate large intracellular vesicles. RAW264.7 macrophages transiently coexpressing ARF6-WT (left) or ARF6-T27N (right) with GFP were sorted by flow cytometry and incubated with IgG-SRBC for 20 min at 37°C, then fixed and processed for transmission EM. SRBCs appear as large electron-dense areas. Cells expressing ARF6-T27N exhibited enlarged electronlucent intracellular compartments, as assessed by direct counting of the number of characteristic enlarged compartments in 30 macrophages. The large intracellular compartments present in ARF6-T27N–positive cells often contained internal membranes (bottom right panel, arrowheads). Data are representative of two independent experiments (sorting and analysis). Bars, 2 μm.

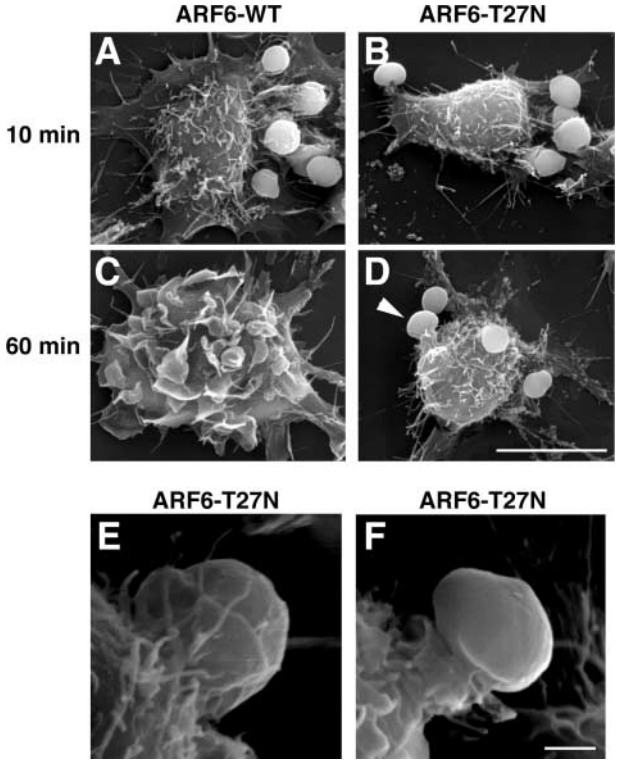

Figure 5. **ARF6-T27N inhibits membrane extension around the particles.** RAW264.7 cells expressing ARF6-WT (A and C) or ARF6-T27N (B and D) were incubated with IgG-SRBC for 10 min (A and B) or 60 min (C and D) at 37°C, then fixed and processed for scanning EM. Arrowhead points to an abortive phagosome. Bar, 10 μm. (E and F) Scanning electron micrographs of macrophages expressing ARF6-T27N incubated with IgG-SRBC for 60 min at 37°C. Bar, 1 μm.

trols membrane recruitment at the site of phagocytosis, rather than actin polymerization. Indeed, polymerized actin was still detected around the nascent phagosomes in ARF6-T27N–expressing cells while there was a default in VAMP3$^+$ membrane accumulation. Thus, our results suggest that ARF6 controls polarized membrane recycling during phagocytosis, whereas actin polymerization would be under the control of Rac/Cdc42 (Castellano et al., 2001; May and Machesky, 2001). In addition, ARF6 also regulates the constitutive recycling of Tf in RAW264.7 cells in the absence of a phagocytic trigger, as previously shown in fibroblasts (D'Souza-Schorey et al., 1995). By contrast, the inhibition of phospholipase A2 lead to a massive accumulation of vesicles specifically to sites of particle attachment (Lennartz et al., 1997). Therefore, arachidonic acid, the product of phospholipase A2, may be needed for the selective docking or fusion of recruited membranes during phagocytosis. Similarly to ARF6, a Rab11 mutant was reported to inhibit Tf recycling and to block phagocytosis (Cox et al., 2000). Thus, both ARF6 and Rab11 GTP-binding proteins participate in the control of Tf recycling and the recruitment of Tf/VAMP3$^+$ endocytic membranes to the macrophage surface during phagocytosis. It is still unclear how ARF6 and Rab11 cooperate and how recycling may be regulated and polarized by a phagocytic signal. ARF6 could control membrane remodeling via two effectors, phospholipase D and phosphatidylinositol 4-phosphate 5-kinase α, which produce phosphatidic acid and phosphatidylinositol (4, 5) bisphosphate, respectively, and are known to modulate vesicular traffic and actin polymerization (Honda et al., 1999; Vitale et al., 2002).

The phagocytic defect induced by dominant-negative ARF6 resembles that observed when PI3K is inhibited in macrophages (Araki et al., 1996; Cox et al., 1999). In both cases, particle recognition at the macrophage surface as well as actin assembly at the contact points were not affected, whereas membrane delivery and extension around the particles were severely inhibited, leading to abortive phagosome formation (Cox et al., 1999; this paper). All these results, together with the fact that the activation of ARNO, an exchange factor for ARF6, depends on PI3K activity (Venkateswarlu et al., 1998), suggest that ARF6- and PI3K-signaling pathways could intersect and cooperate in order to allow membrane extension. Furthermore, the observation that Rac is activated before ARF6 and Cdc42 in RAW264.7 cells may indicate that Rac is upstream of ARF6 and Cdc42, corroborating previously published results on macrophage spreading (Zhang et al., 1999). However, it has to be noted that distinct activation profiles for Rac and ARF6 were documented during scattering of epithelial cells (D'Souza-Schorey et al., 1997; Palacios and D'Souza-Schorey, 2003). Furthermore, concerted but parallel activations have also been described recently for Rac and Cdc42 during phagocytosis (Patel et al., 2002). The signaling cascade leading to the activation of ARF6 during phagocytosis still has to be dissected. Several exchange factors have been described for ARF6 (Chavrier and Goud, 1999; Jackson and Casanova, 2000), including ARNO and EFA6 family members (Derrien et al., 2002) that could be activated after engagement of FcR during phagocytosis.

There are multiple sources of intracellular membrane that contribute to pseudopod formation in phagocytes. Indeed, lysosomes and the ER have recently been shown to be recruited to nascent phagosomes (Muller-Taubenberger et al., 2001; Aderem, 2002; Allen et al., 2002; Gagnon et al., 2002; Tapper et al., 2002). It is not clear if these compartments have distinct functions in the phagosome formation and maturation processes that lead to the degradation of the ingested particles, and eventually, to the presentation of derived antigens. The question also remains open whether and how exocytosis of these different compartments is coordinated. To control membrane delivery during phagocytosis, ARF6 could act at different stages of the process, i.e., directionality for vesicle movement, vesicle budding, docking, or fusion with the forming phagosome. Cell spreading and motility, which are controlled by ARF6, are also thought to depend on polarized insertion of membrane at specific sites of the plasma membrane (Turner and Brown, 2001). The characterization of the molecular basis of ARF6 function in these related cellular functions will be a major challenge for the next years.

Materials and methods

Plasmids and reagents

The ARF6-WT– and ARF6-T27N–expressing plasmids have been described previously (D'Souza-Schorey et al., 1998). The expression vectors encoding the dominant inhibitory domain of Eps15 (pEGFPC2Eps15DIII) or a control construct (pEGFPC2Eps15DIIIΔ2; Benmerah et al., 2000) were provided by Dr. A. Benmerah (INSERM U567-CNRS UMR8104, Institut Cochin, Paris, France). The plasmid encoding GFP-VAMP3 was a gift of Dr. T. Galli (INSERM U536, Institut du Fer-à-Moulin, Paris, France). The plasmid encoding the GST-fused Rac-interactive binding domain of PAK1 (GST-CRIB) was obtained from Dr. A. Hall (University College London, London, UK) The pGEX4T1 (Amersham Biosciences) vector encoding GST-$GGA3_{1–226}$ was constructed by PCR from human GGA3 cDNA (short isoform) subcloned into pcDNA3.1 (Boman et al., 2000; a gift of Dr. R.A. Kahn, Emory University School of Medicine, Atlanta, GA).

The anti-HA mAbs (clone 3F10) were purchased from Roche, the anti-ARF6 pAbs were a gift from Dr. V.W. Hsu (Brigham and Woman's Hospital, Boston, MA), monoclonal anti-Rac1 antibodies were provided by Dr. T. Azuma (Harvard Medical School, Boston, MA), and rabbit anti-Cdc42 antibodies were homemade. Fluorochrome-labeled antibodies or reagents were as follows: Texas red–labeled human Tf; Alexa® 633–labeled human Tf, Alexa® 633–labeled phalloidin, and Alexa® 350–coupled phalloidin (Molecular Probes, Inc.); Cy3-labeled $F(ab')_2$ anti–rabbit IgG and Cy2-labeled $F(ab')_2$ anti–rat IgG (Jackson ImmunoResearch Laboratories); and HRP-coupled anti–rabbit or anti–rat IgG (Sigma-Aldrich). Purified rabbit anti-SRBC IgG (ICN Biomedicals) were coupled to Cy5 with the Fluoro-Link™ Cy™5 labeling kit (Amersham Biosciences). GST-fused $GGA3_{1–226}$ and GST-CRIB were prepared as described previously (Dubois et al., 2001), except that it was purified on GST bead columns, directly dialyzed against 20 mM Tris (pH 7.4), 2 mM EDTA, 100 mM NaCl, 2 mM β-mercaptoethanol, and 10% glycerol, aliquoted, and stored at −80°C.

Cell culture, Tf uptake, and transfection

RAW264.7 macrophages were grown in complete medium, consisting of RPMI 1640–glutamax supplemented with 10% FCS (Biomedia) and 10 mM Hepes, 1 mM sodium pyruvate, and 50 μM β-mercaptoethanol (all from GIBCO BRL). 60 nM Texas red-Tf was internalized into cells for 30 min at 37°C as described previously (Niedergang et al., 1995). Cells were transfected by electroporation with the Optimix kit (EquiBio). Routinely, one 100-mm plate of cells grown to subconfluence and 20 μg plasmid were used for each transfection (20 μg plasmid of interest plus 10 μg plasmid encoding GFP for cotransfections). The cells were electroporated in 0.4-cm cuvettes (EquiBio) at 240 V, 950 μF in an electroporation apparatus (Gene Pulser II; Bio-Rad Laboratories), then immediately resuspended in complete culture medium and plated in 100-mm dishes containing 12-mm coverslips. Efficiency of transfection was 10–40%. To generate stable clones expressing GFP-VAMP3, transfected cells were sorted on a FACS-Vantage™ cell sorter (Becton Dickinson), cloned by limiting dilution, and cultivated in the presence of 1 mg/ml G418 in complete medium.

Preparation of SRBC and phagocytosis assays

SRBCs were purified from sheep blood (Unité Commune d'Expérimentation Animale, Institut National de la Recherche Agronomique, Jouy-en-Josas, France). The blood was diluted two times in Alsever's buffer (23 mM sodium citrate, 114 mM glucose, 72 mM NaCl, and 2.6 mM citric acid, pH 6) and centrifuged on a ficoll gradient (Ficoll Paque Plus™, Amersham Biosciences; blood:ficoll = 1:3, vol/vol) at 500 *g* without brake. RBCs were collected from the pellet and washed three times in Alsever's buffer. The solution was adjusted to 3.6×10^9 cells/ml in the same buffer and conserved at 4°C.

Phagocytosis was performed essentially as described previously (Patel et al., 2000). SRBCs opsonized with IgG were resuspended in prewarmed phagocytosis medium (serum-free complete RPMI 1640) and distributed on the cells grown on coverslips (SRBC:macrophage ratio of 10). Phagocytosis was synchronized by centrifugation for 2 min at 400 *g*, and the kinetics was started by incubating the plates at 37°C, 7% CO_2. At different time points, the cells were washed and fixed using standard protocols for immunofluorescence (Niedergang et al., 1995) or electron microscopy (Niedergang et al., 2000).

Immunofluorescence

Cells were fixed in 4% PFA-PBS for 45 min at 4°C, incubated for 10 min with 50 mM NH_4Cl^- PBS, washed, and incubated with Cy3-labeled $F(ab')_2$ anti–rabbit IgG antibodies in 2% FCS/PBS (PBS-FCS) for 45 min at RT to detect external IgG-SRBC. Internalized IgG-SRBC is protected from this labeling and appears swollen in phase contrast. Cells were then washed twice in PBS-FCS and incubated for 45 min with the anti-HA antibodies in the permeabilizing buffer (PBS-FCS/0.05% saponin) to detect transfected cells. Subsequent steps were performed at RT in permeabilizing buffer. After two washes, cells were incubated with Cy2- or Cy3-coupled anti–rat antibodies and Alexa® 350–phalloidin in permeabilizing buffer, washed three times in the same buffer and twice in PBS, and mounted on microscope slides in 100 mg/ml Mowiol, 25% (vol/vol) glycerol, and 100 mM Tris, pH 8. The samples were examined under a confocal microscope (model SP2; Leica) equipped with Ar and He/Ne lasers. Each fluorescent signal was acquired separately. Serial optical sections were recorded at

0.3-μm intervals with a 100×, 1.4 NA objective. Alternatively, the cells were examined under an inverted microscope (model DMIRE2; Leica) equipped with a cooled interlined CCD camera (CoolSNAP HQ™; Roper Scientific). The Z-positioning was accomplished by a piezo-electric motor, and deconvolution was performed by the new three-dimensional deconvolution module from MetaMorph® (Universal Imaging Corp.), using the fast iterative constrained PSF-based algorithm.

EM

Phagocytosis was performed as described earlier in Materials and methods, except that at different time points, cells were washed in phagocytosis medium at RT and fixed in 2.5% glutaraldehyde in 0.066 M cacodylate buffer (Niedergang et al., 2000). For scanning EM, samples were examined with a microscope (model JSM 840A, JEOL; Centre InterUniversitaire de Microscopie Electronique, Université Paris 6, Paris, France) at an accelerating voltage of 17 kV. For transmission EM, ultrathin sections of plastic-embedded macrophages were counterstained with 2% uranyl acetate in methanol for 5 min and viewed and photographed with a microscope (CM120 Twin; Philips) at 60 kV. The negatives were scanned with a scanner (HiScan; Eurocore) and processed with Adobe Photoshop® 5.5 software. Relative quantitation of intracellular vesicles was performed directly under the electron microscope by counting the number of characteristic enlarged compartments in 30 macrophages.

Quantitative analysis of phagocytosis

The number of internalized SRBCs was counted in 50 cells randomly chosen on the coverslips, and the phagocytic index (i.e., the mean number of phagocytosed SRBCs per cell) was calculated (usually 2–5). The index obtained for transfected cells was divided by the index obtained for control nontransfected cells and expressed as a percentage of control cells. We also counted the number of cell-associated (bound + internalized) SRBCs, calculated the association index (mean number of associated SRBCs per cell), and expressed it as percentage of control nontransfected cells. To quantitate actin and membrane-phagocytic cup profiles, we scored the accumulations of GFP-VAMP3 and F-actin in 50 cells randomly chosen on the coverslips, and calculated an accumulation index (i.e., the mean number of accumulations per cell). The index obtained for ARF6-expressing cells was divided by the index obtained for control nontransfected cells and was expressed as a percentage of the latter. Alternatively, cells were analyzed by flow cytometry as described previously (Coppolino et al., 2002).

Tf recycling

Transfected cells were scraped, washed once in endocytosis medium (serum-free complete RPMI 1640 medium supplemented with 1 mg/ml BSA), and incubated for 45 min at 37°C in the presence of 15 μg/ml Alexa® 633-Tf. The cells were then placed on ice, washed in cold endocytosis medium, and resuspended in prewarmed complete RPMI 1640 medium. At the indicated times, aliquots of cells were taken and diluted in PBS/2% FCS on ice. The cells were then pelleted and analyzed on a FACSCalibur™ system (Becton Dickinson), measuring the GFP and the Alexa® 633 fluorescences. At least 10,000 GFP-positive cells were acquired, and the mean Alexa® 633 fluorescence was calculated for GFP-negative and -positive cells. The values obtained at each time point were expressed as a percentage of the value measured at t = 0.

Pull-down assay and determination of the activation of ARF6

6–8 million of RAW264.7 cells grown at subconfluence were used for each point of the phagocytosis kinetics. Cells were scraped and resuspended in phagocytosis medium. Phagocytosis was performed in suspension, initiated by the addition of IgG-SRBC in prewarmed phagocytosis medium (SRBC:macrophage ratio of 10), and synchronized by centrifugation in a microfuge. After incubation at 37°C for different time points, cells were centrifuged at 13,000 *g* for 15 s, the supernatant was removed, and cells were lysed on ice in lysis buffer as described previously (Patel et al., 2002). Precipitation was performed in the presence of 0.5% BSA with GST (25 μg), GST-GGA3$_{1–226}$ (50 μg), or GST-CRIB (50 μg) at 4°C and revealed by Western blotting.

We thank Drs. Jean-Baptiste Sibarita and Vincent Fraisier for their expertise in developing and performing wide-field fluorescence microscopy and deconvolution; Dr. Michèle Grasset for assistance with scanning EM; Danielle Rouillard for cell sorting; Dr. Emmanuelle Caron for initial advice on phagocytosis experiments; and Jean-François Alkombre for collecting samples of sheep blood. We are grateful to Dr. Andrés Alcover for critical reading of the manuscript.

This work was supported by institutional funding from the CNRS and grants from the Institut Curie, the Programme de Recherche Fondamentale en Microbiologie et Maladies Infectieuses et Parasitaires, and the Ligue Nationale contre le Cancer (Equipe Labelisée). T. Dubois is the recipient of a post-doctoral fellowship from Association pour la Recherche sur le Cancer.

Submitted: 11 October 2002
Revised: 1 May 2003
Accepted: 1 May 2003

References

Aderem, A. 2002. How to eat something bigger than your head. *Cell.* 110:5–8.

Aderem, A., and D.M. Underhill. 1999. Mechanisms of phagocytosis in macrophages. *Annu. Rev. Immunol.* 17:593–623.

Allen, L.A., C. Yang, and J.E. Pessin. 2002. Rate and extent of phagocytosis in macrophages lacking VAMP3. *J. Leukoc. Biol.* 72:217–221.

Altschuler, Y., S.-H. Liu, L. Katz, K. Tang, S. Hardy, F. Brodsky, G. Apodaca, and K. Mostov. 1999. ADP-ribosylation factor 6 and endocytosis at the apical surface of Madin-Darby canine kidney cells. *J. Cell Biol.* 147:7–12.

Araki, N., M.T. Johnson, and J.A. Swanson. 1996. A role for phosphoinositide 3-kinase in the completion of macropinocytosis and phagocytosis by macrophages. *J. Cell Biol.* 135:1249–1260.

Bajno, L., X.-R. Peng, A.D. Schreiber, H.-P. Moore, W.S. Trimble, and S. Grinstein. 2000. Focal exocytosis of VAMP3-containing vesicles at sites of phagosome formation. *J. Cell Biol.* 149:697–705.

Benmerah, A., V. Poupon, N. Cerf-Bensussan, and A. Dautry-Varsat. 2000. Mapping of Eps15 domains involved in its targeting to clathrin-coated pits. *J. Biol. Chem.* 275:3288–3295.

Boman, A.L., C. Zhang, X. Zhu, and R.A. Kahn. 2000. A family of ADP-ribosylation factor effectors that can alter membrane transport through the trans-Golgi. *Mol. Biol. Cell.* 11:1241–1255.

Booth, J.W., W.S. Trimble, and S. Grinstein. 2001. Membrane dynamics in phagocytosis. *Semin. Immunol.* 13:357–364.

Castellano, F., P. Chavrier, and E. Caron. 2001. Actin dynamics during phagocytosis. *Semin. Immunol.* 13:347–355.

Chavrier, P., and B. Goud. 1999. The role of ARF and Rab GTPases in membrane transport. *Curr. Opin. Cell Biol.* 11:466–475.

Coppolino, M.G., R. Dierckman, J. Loijens, R.F. Collins, M. Pouladi, J. Jongstra-Bilen, A.D. Schreiber, W.S. Trimble, R. Anderson, and S. Grinstein. 2002. Inhibition of phosphatidylinositol-4-phosphate 5-kinase Iα impairs localized actin remodeling and suppresses phagocytosis. *J. Biol. Chem.* 277:43849–43857.

Cox, D., C.C. Tseng, G. Bjekic, and S. Greenberg. 1999. A requirement for phosphatidylinositol 3-kinase in pseudopod extension. *J. Biol. Chem.* 274:1240–1247.

Cox, D., D.J. Lee, B.M. Dale, J. Calafat, and S. Greenberg. 2000. A Rab11-containing rapidly recycling compartment in macrophages that promotes phagocytosis. *Proc. Natl. Acad. Sci. USA.* 97:680–685.

D'Souza-Schorey, C., G. Li, M.I. Colombo, and P.D. Stahl. 1995. A regulatory role for ARF6 in receptor-mediated endocytosis. *Science.* 267:1175–1178.

D'Souza-Schorey, C., R.L. Boshans, M. MacDonough, P.D. Stahl, and L. Van Aelst. 1997. A role for POR1, a Rac-interacting protein, in ARF6-mediated cytoskeletal rearrangements. *EMBO J.* 16:5445–5454.

D'Souza-Schorey, C., E. van Donselaar, V.W. Hsu, C. Yang, P.D. Stahl, and P.J. Peters. 1998. ARF6 targets recycling vesicles to the plasma membrane: insights from an ultrastructural investigation. *J. Cell Biol.* 140:603–616.

Dautry-Varsat, A., A. Ciechanover, and H.F. Lodish. 1983. pH and the recycling of transferrin during receptor-mediated endocytosis. *Proc. Natl. Acad. Sci. USA.* 80:2258–2262.

Derrien, V., C. Couillault, M. Franco, S. Martineau, P. Montcourrier, R. Houlgatte, and P. Chavrier. 2002. A conserved C-terminal domain of EFA6-family ARF6-guanine nucleotide exchange factors induces lengthening of microvilli-like membrane protrusions. *J. Cell Sci.* 115:2867–2879.

Dubois, T., P. Kerai, E. Zemlickova, S. Howell, T.R. Jackson, K. Venkateswarlu, P.J. Cullen, A.B. Theibert, L. Larose, P.J. Roach, and A. Aitken. 2001. Casein kinase I associates with members of the centaurin-α family of phosphoinositol 3,4,5-trisphosphate-binding proteins. *J. Biol. Chem.* 276: 18757–18764.

Gagnon, E., S. Duclos, C. Rondeau, E. Chevet, P.H. Cameron, O. Steele-Mortimer, J. Paiement, J.J. Bergeron, and M. Desjardins. 2002. Endoplasmic reticulum-mediated phagocytosis is a mechanism of entry into macrophages. *Cell.* 110:119–131.

Gold, E.S., D.M. Underhill, N.S. Morrissette, J. Guo, M.A. McNiven, and A. Ad-

erem. 1999. Dynamin 2 is required for phagocytosis in macrophages. *J. Exp. Med.* 190:1849–1856.

Gold, E.S., N.S. Morrissette, D.M. Underhill, J. Guo, M. Bassetti, and A. Aderem. 2000. Amphiphysin IIm, a novel amphiphysin II isoform, is required for macrophage phagocytosis. *Immunity.* 12:285–292.

Greenberg, S., and S. Grinstein. 2002. Phagocytosis and innate immunity. *Curr. Opin. Immunol.* 14:136–145.

Hackam, D.J., O.D. Rotstein, C. Sjolin, A.D. Schreiber, W.S. Trimble, and S. Grinstein. 1998. v-SNARE-dependent secretion is required for phagocytosis. *Proc. Natl. Acad. Sci. USA.* 95:11691–11696.

Holevinsky, K.O., and D.J. Nelson. 1998. Membrane capacitance changes associated with particle uptake during phagocytosis in macrophages. *Biophys. J.* 75:2577–2586.

Honda, A., M. Nogami, T. Yokoseki, M. Yamazaki, H. Nakamura, H. Watanabe, K. Kawamoto, K. Nakayama, A.J. Morris, M.A. Frohman, and Y. Kanaho. 1999. Phosphatidylinositol 4-phosphate 5-kinase α is a downstream effector of the small G protein ARF6 in membrane ruffle formation. *Cell.* 99:521–532.

Jackson, C.L., and J.E. Casanova. 2000. Turning on ARF: the Sec7 family of guanine-nucleotide-exchange factors. *Trends Cell Biol.* 10:60–67.

Lennartz, M.R., A.F.C. Yuen, S. McKenzie Masi, D.G. Russel, K.F. Buttle, and J.J. Smith. 1997. Phospholipase A_2 inhibition results in sequestration of plasma membrane into electronlucent vesicles during IgG-mediated phagocytosis. *J. Cell Sci.* 110:2041–2052.

May, R.C., and L.M. Machesky. 2001. Phagocytosis and the actin cytoskeleton. *J. Cell Sci.* 114:1061–1077.

Muller-Taubenberger, A., A.N. Lupas, H. Li, M. Ecke, E. Simmeth, and G. Gerisch. 2001. Calreticulin and calnexin in the endoplasmic reticulum are important for phagocytosis. *EMBO J.* 20:6772–6782.

Niedergang, F., A. Hémar, C.R.A. Hewitt, M.J. Owen, A. Dautry-Varsat, and A. Alcover. 1995. The *Staphylococcus aureus* enterotoxin B superantigen induces specific T cell receptor down-regulation by increasing its internalization. *J. Biol. Chem.* 270:12839–12845.

Niedergang, F., J.-C. Sirard, C. Tallichet Blanc, and J.-P. Kraehenbuhl. 2000. Entry and survival of *Salmonella typhimurium* in dendritic cells and presentation of recombinant antigens do not require macrophage-specific virulence factors. *Proc. Natl. Acad. Sci. USA.* 97:14650–14655.

Palacios, F., and C. D'Souza-Schorey. 2003. Modulation of Rac1 and ARF6 activation during epithelial cell scattering. *J. Biol. Chem.* 278:17395–17400.

Palacios, F., L. Price, J. Schweitzer, J.G. Collard, and C. D'Souza-Schorey. 2001. An essential role for ARF6-regulated membrane traffic in adherens junction turnover and epithelial cell migration. *EMBO J.* 20:4973–4986.

Patel, J.C., A. Hall, and E. Caron. 2000. Rho GTPases and macrophage phagocytosis. *Methods Enzymol.* 325:462–473.

Patel, J.C., A. Hall, and E. Caron. 2002. Vav regulates activation of Rac but not Cdc42 during FcγR-mediated phagocytosis. *Mol. Biol. Cell.* 13:1215–1226.

Perry, D.G., G.L. Daugherty, and W.J. Martin, Ii. 1999. Clathrin-coated pit-associated proteins are required for alveolar macrophage phagocytosis. *J. Immunol.* 162:380–386.

Radhakrishna, H., and J.G. Donaldson. 1997. ADP-ribosylation factor 6 regulates a novel plasma membrane recycling pathway. *J. Cell Biol.* 139:49–61.

Radhakrishna, H., R.D. Klausner, and J.G. Donaldson. 1996. Aluminum fluoride stimulates surface protrusions in cells overexpressing the ARF6 GTPase. *J. Cell Biol.* 134:935–947.

Santy, L.C., and J.E. Casanova. 2001. Activation of ARF6 by ARNO stimulates epithelial cell migration through downstream activation of both Rac1 and phospholipase D. *J. Cell Biol.* 154:599–610.

Tapper, H., W. Furuya, and S. Grinstein. 2002. Localized exocytosis of primary (lysosomal) granules during phagocytosis: role of Ca^{2+}-dependent tyrosine phosphorylation and microtubules. *J. Immunol.* 168:5287–5296.

Tse, S.M.L., W. Furuya, E.S. Gold, A.D. Schreiber, K. Sandvig, R.D. Inman, and S. Grinstein. 2003. Differential role of actin, clathrin, and dynamin in Fcγ receptor-mediated endocytosis and phagocytosis. *J. Biol. Chem.* 278:3331–3338.

Turner, C.E., and M.C. Brown. 2001. Cell motility: ARNO and ARF6 at the cutting edge. *Curr. Biol.* 11:R875–R877.

Venkateswarlu, K., P.B. Oatey, J.M. Tavare, and P.J. Cullen. 1998. Insulin-dependent translocation of ARNO to the plasma membrane of adipocytes requires phosphatidylinositol 3-kinase. *Curr. Biol.* 8:463–466.

Vitale, N., S. Chasserot-Golaz, Y. Bailly, N. Morinaga, M.A. Frohman, and M.F. Bader. 2002. Calcium-regulated exocytosis of dense-core vesicles requires the activation of ADP-ribosylation factor (ARF)6 by ARF nucleotide binding site opener at the plasma membrane. *J. Cell Biol.* 159:79–89.

Zhang, Q., D. Cox, C.-C. Tseng, J.G. Donaldson, and S. Greenberg. 1998. A requirement for ARF6 in Fcγ receptor-mediated phagocytosis in macrophages. *J. Biol. Chem.* 273:19977–19981.

Zhang, Q., J. Calafat, H. Janssen, and S. Greenberg. 1999. ARF6 is required for growth factor- and Rac-mediated membrane ruffling in macrophages at a stage distal to Rac membrane targeting. *Mol. Cell. Biol.* 19:8158–8168.